Bolometric Measurements of Radiated Power Profiles from Initial NBI Heated Plasmas in the Large Helical Device

B. J. Peterson, K. Y. Watanabe, M. Osakabe, R. Sakamoto, Y. Xu[1], S. Sudo, H. Idei, S. Kado, S. Kubo, J. Miyazawa, S. Morita, K. Narihara, S. Sakakibara, K. Tanaka, T. Tokuzawa, K. Tsumori, H. Yamada, A. Komori, O. Kaneko, K. Kawahata, N. Ohyabu, O. Motojima, M. Fujiwara and LHD Experimental Groups I and II

National Institute for Fusion Science, Toki-shi, Gifu-ken 509-5292, Japan
[1]University of Science and Technology of China, Hefei, Anhui 230026, P. R. China

1. Introduction

During the second experimental cycle of the Large Helical Device [1] (B_t = 1.5 T, R/a = 3.75/0.6 m, l/m = 2/10) measurements using metal film bolometers were made of the power radiated from NBI (hydrogen, 100kV, 1 - 2.5 MW) heated plasmas (n_e = 0.6 – 7.0 x 10^{19}/m^3, T_e = 0.5 - 2keV, T_i = 0.5 - 2keV).

2. Bolometer arrays and inversion technique

Two arrays of metal film bolometers [2] were installed on the Large Helical Device for the second experimental campaign. The bolometer sight lines and magnetic flux surfaces for β = 0.32% (calculated with VMEC) are included in a CAD model as shown in Figure 1. The blackened bolometers were calibrated using a helium neon laser by determining the thermal decay time, τ, and the sensistivity, K, and to give the brightness, P_{rad} , from the signal voltage, V_b, using Equation 1.

$$P_{rad} = \frac{1}{K}\left(V_b + \tau \frac{\partial V_b}{\partial t}\right) \qquad (1)$$

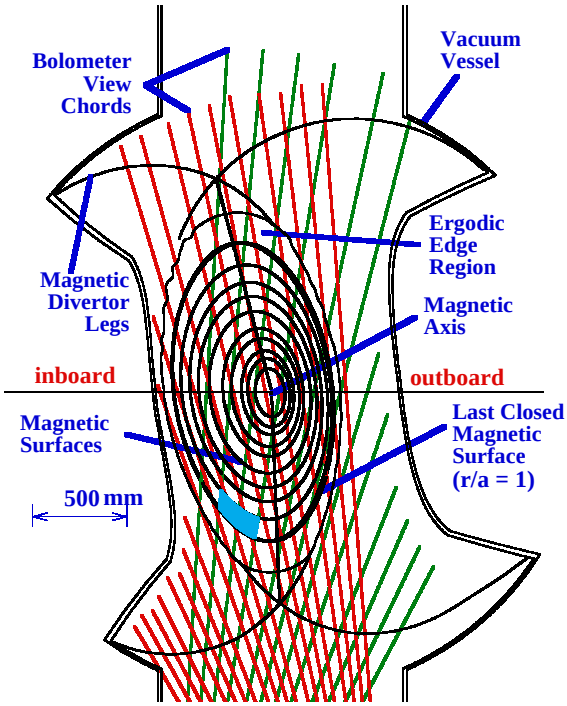

Figure 1 CAD drawing showing cross-section of LHD with bolometer sight lines (green and red) and magnetic surfaces (black). A sample intersection volume, V_{ij}, is shown shaded (cyan).

The surfaces were divided by lines which were drawn arbitrarily between the magnetic axis and the X-points. Doing so permits the separate evaluation of the inboard and outboards sides

of the radiation profiles. This divides the plasma into 19 distinct regions through which 19 bolometer viewing chords pass. Using the CAD model, the intersecting volumes, V_{ij}, (between the bolometer viewing chord volume and the volume between surfaces as shown by the shaded region in Figure 1) are calculated for each combination of plasma region and viewing chord (detector channel). The solid angle of the detector, Ω_{ij}, is also calculated for each of these intersecting volumes. Then a system of equations is written for the detector power, P_i, and region emissivity, S_j, as

$$P_i = \sum_j \frac{\Omega_{ij}}{4\pi} V_{ij} S_j = \sum_j T_{ij} S_j . \qquad (2)$$

The emissivities are then solved for by inverting the two dimensional matrix T using Singular Value Decomposition (SVD) and back substituting with the singularities removed [3].

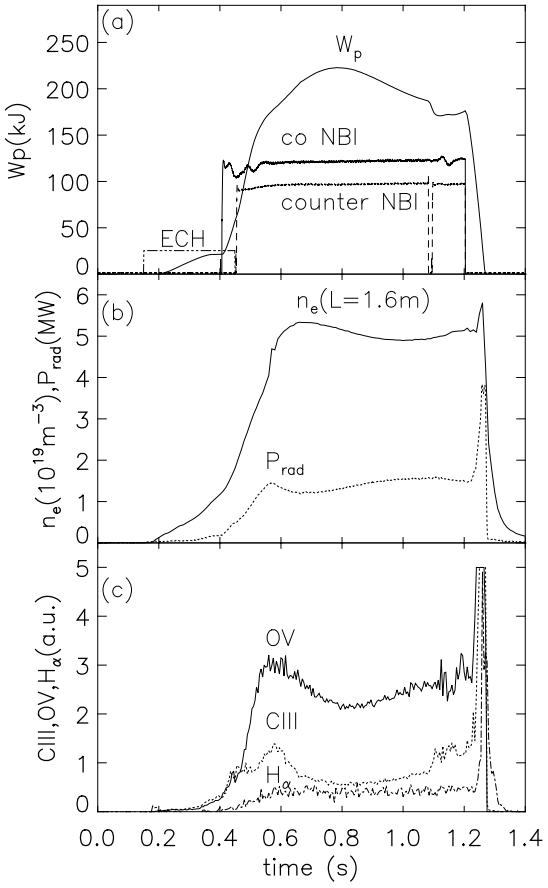

Figure 2 Shot 3700 Summary (a) ECH and NBI timing and diamagnetic stored energy. (b) line-averaged density and total radiated power. (c) spectroscopy signals from CIII, OV and Hα.

3. Radiated power profiles with helium and hydrogen puffing

Figure 2 shows the shot summary for a typical discharge using helium puffing during the first half of LHD's second experimental cycle. The plasma is formed by ECH and then heated by NBI to a steady state condition until the beams turn off and the plasma terminates in radiative thermal decay. The similarity between the total radiated power signal and the carbon and oxygen impurity radiation signals is consistent with spectroscopic information that they are the major radiating impurities. Figure 3 shows the radiated power profile evolution for the same shot during and after NBI.

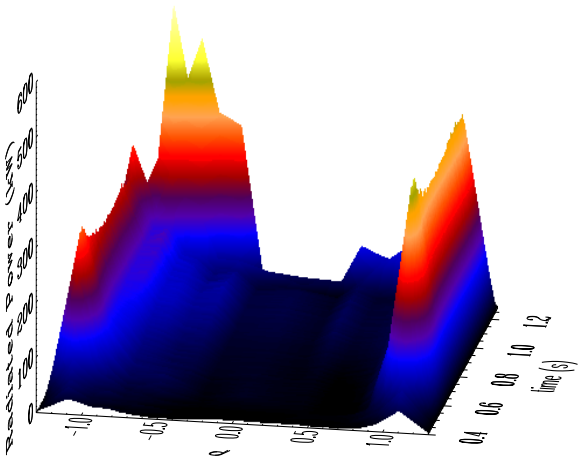

Figure 3 Radiated power profile evolution for Shot 3700 using helium puffing.

This shows that 40 to 50% of the radiated power is coming from the edge ergodic region ($\rho > 1$). At the end of the discharge after the NBI terminates, the radiation increases dramatically and becomes very asymmetric on the inboard side.

Figure 4 shows the discharge summary for a shot with hydrogen puffing. In this case the total radiated power seen in Figure 4b slowly increases from 50% of the NBI-deposited power (as calculated from NBI port-thru and shine-thru powers) at the beginning of the discharge until it exceeds the deposited power as the plasma experiences radiative thermal collapse. In Figure 5 the emissivisty profile evolution for this shot is shown. The profile during the steady state portion of the discharge is hollow as was the case with helium puffing but is terminated with a radiative collapse that is quite symmetric. After the collapse a strong carbon afterglow is observed in the region $\rho < 0.5$, probably due to the increase in carbon impurities as a result of the poorly absorbed neutral beam hitting the carbon-tiled beam dump.

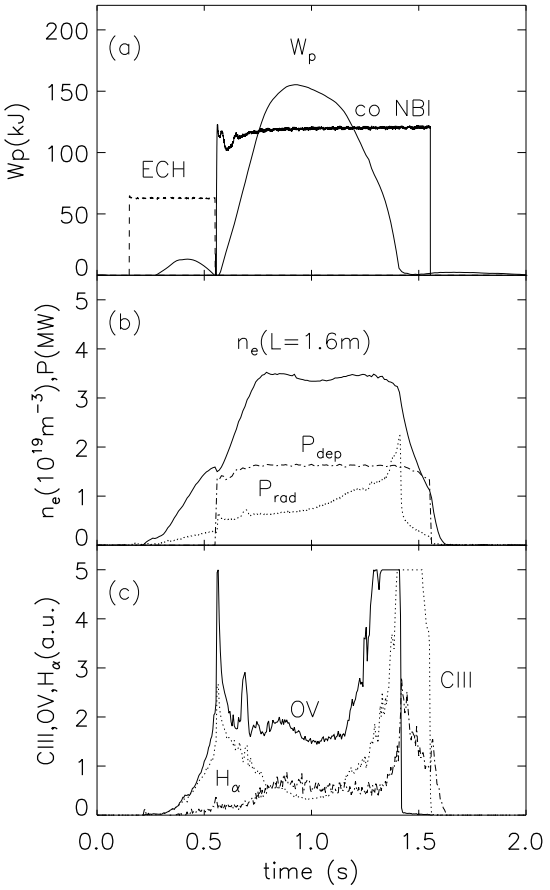

Figure 4 Shot 4621 Summary (a) ECH and NBI timing and diamagnetic stored energy. (b) line-averaged density, deposited NBI power and total radiated power. (c) spectroscopy signals from CIII, OV and Hα.

4. Emissivity profiles with pellet injection

In Figure 6 the shot summary is shown for a discharge with a hydrogen pellet injected at $t = 0.55$ seconds. The pellet contains 9 x 10^{20} atoms and is injected at a speed of 1 km/s. The radiation profile evolution during the NBI heating phase is shown in Figure 7. Immediately after the pellet is injected a strong peak is seen in the outboard ergodic region which then moves to the inboard side. As the

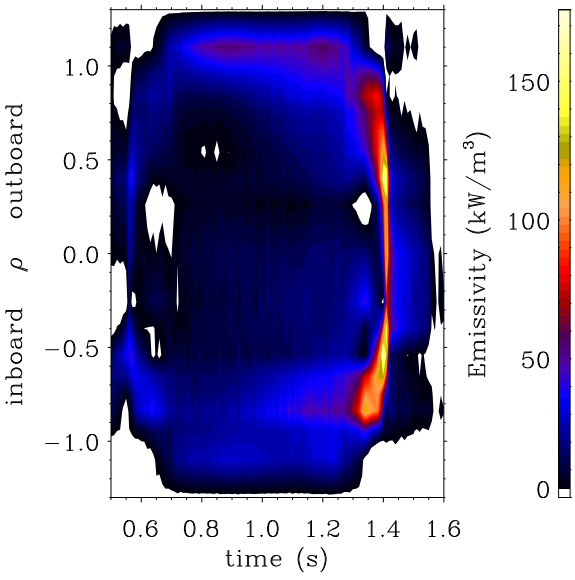

Figure 5 Shot 4621 emissivity profile evolution during and after NBI with hydrogen puffing.

discharge progresses radiation is observed first from the $\rho = 0.4$ region and then from the magnetic axis.

5. Summary

Radiated power profiles have been obtained during initial NBI discharges in LHD from measurements with metal film bolometer arrays using an SVD inversion technique. During the steady state portions of discharges using hydrogen puffing and of those using helium puffing very hollow radiated power profiles are observed with up to 50% of the radiated power comes from the ergodic edge region outside of the last closed magnetic surface ($\rho > 1$). Radiated power fractions range from 50% to more than 100% in cases leading to radiative thermal collapse. During the thermal decay in the NBI afterglow the plasma radiates strongly from the inboard side. After pellet injection the peak in the emissivity profile starts from the edge ergodic region on the outboard side, switches to the edge region on the inboard side, then moves towards the axis.

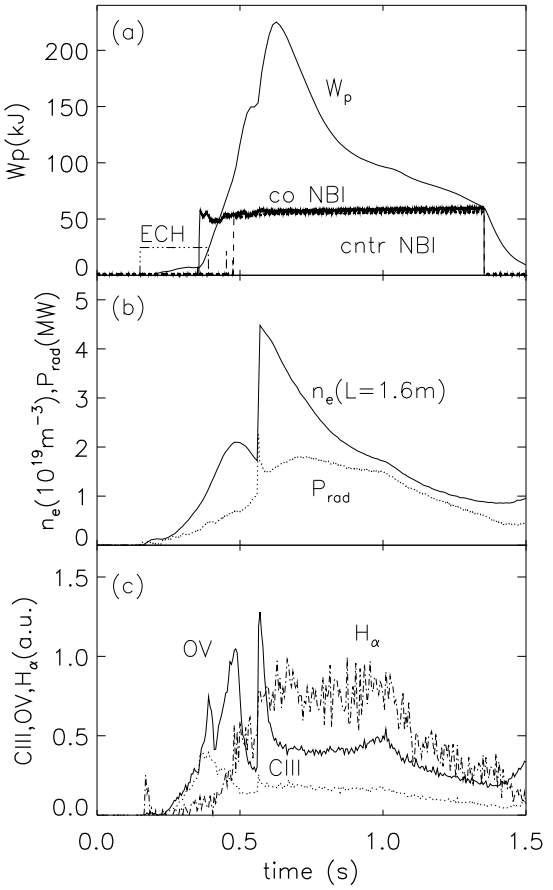

Figure 6 Shot 6121 Summary (a) ECH and NBI timing and diamagnetic stored energy. (b) line-averaged density and total radiated power. (c) spectroscopy signals from CIII, OV and Hα.

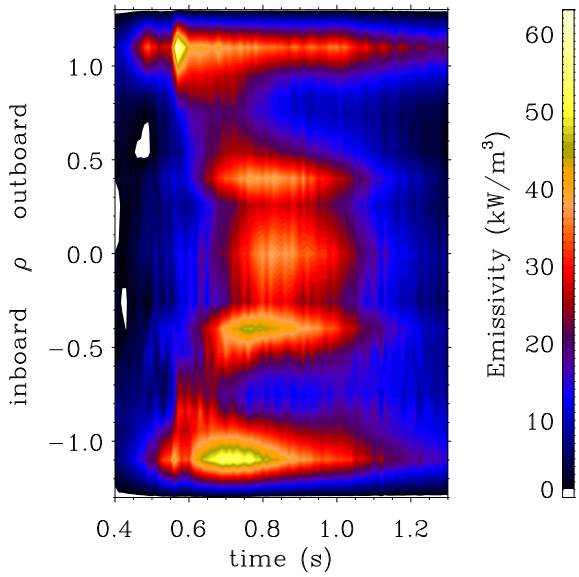

Figure 7 Shot 6121 emissivity profile evolution during NBI with hydrogen pellet injection at t = 0.55 seconds.

References

[1] O. Motojima, H. Yamada, A. Komori, *et al.*, Physics of Plasmas, **6** (1999) 1843.

[2] K. F. Mast, *et al.*, Rev. Sci. Instrum. **62** (1991) 744.

[3] W. H. Press, *et al.*, Numerical Recipes, the Art of Scientific Computing, (Cambridge University Press, Cambridge, 1986), pp. 52-58.